# Optimizing the Form Error of Al6061 Spherical Surfaces in Single-Point Diamond Turning Using Particle Swarm Optimization Algorithm

## Do Manh Tung<sup>1</sup>, Bui Kim Hoa<sup>2</sup>, Hoang Nghia Duc<sup>2</sup>, Nguyen Kim Hung<sup>2</sup>, Ngo Viet Hung<sup>2</sup>, Duong Xuan Bien<sup>2, \*</sup>, Chu Anh My<sup>2</sup>

<sup>1</sup>Faculty of Mechanical Engineering, Le Quy Don Technical University, Ha Noi, Vietnam
<sup>2</sup> Technology Center, Le Quy Don Technical University, Ha Noi, Vietnam

\*Corresponding author email: duongxuanbien@lqdtu.edu.vn

#### **Abstract**

The paper investigates optimizing form accuracy in Al6061 spherical surface (SS) machining through single-point diamond turning (SPDT) with the swarm optimization (PSO) algorithm. The optimization problem is implemented on the basis of building the relationship between profile accuracy or form error (FE) with cutting parameters including spindle speed (n-rev/min), feed rate (f-mm/min), and depth of cut (ap- $\mu$ m). Based on the data collection from 15 experiments in the Box-Behnken (BB) model with the specialized software Design Expert support, the modeling results show a high agreement between the predicted data and the actual measured values with high reliability ( $R^2 = 0.9428$ ). By using the PSO algorithm, the optimal FE value of 0.95  $\mu$ m was found, corresponding to the technological parameter set of n equal 1746 rev/min, f equal 5 mm/min, and ap equal 8  $\mu$ m. This research significantly lays the foundation for controlling, predicting, and optimizing the FE factor of SS, particularly for Al6061 material and generally for other materials. Moreover, these results will further enhance the SPDT machining of more complex surfaces and reduce optical errors.

Keywords: SPDT, form error, PSO, Al6061.

#### 1. Introduction

Ultra-precision machining (UPM) is a mechanical machining technology that achieves extremely high precision and surface finish. The roughness values typically reach a few nanometers or less. This technology is mainly applied in industries that require high surface quality and strict tolerances, such as aerospace, electronics, medical, and optics. Some UPM methods include ultra-precision grinding [1], ultraprecision milling [2], and ultra-precision laser machining [3]. Ultra-precision turning (UPT) [4] is a typical method for machining lens surfaces and molds for lenses in the field of optics. UPT technology can process various types of rotationally symmetric and asymmetric surfaces and can handle difficult-tomachine optical materials such as glass, Ge crystals, ZnSe, CaF<sub>2</sub>, or Silicon, as well as non-ferrous metals like aluminum and copper alloys. In addition, UPT can create surfaces with roughness in the range of a few nanometers, with form error (FE) of less than a few micrometers. UPT can also process lenses with complex shapes, such as aspheric lenses, diffractive lenses, or freeform surfaces.

In optics, surfaces play a crucial role in the transmission and control of light. The FE and roughness of these surfaces directly affect the performance and quality of optical devices such as lenses, mirrors, prisms, and optical sensors. Typical optical surface types such as spherical surfaces [5], aspherical surfaces [6], and

diffraction surfaces [7]. Research on spherical lens surfaces is crucial for controlling and optimizing optical properties like convergence, divergence, and light transmission. The accuracy and quality of the SS directly affect the performance of the optical system, especially in devices that require high precision such as telescopes, microscopes, and medical equipment.

Assessing surface machining quality, especially in the fields of optics and precision mechanics, requires several important technical criteria. The FE is the most important factor. It is the error that measures the deviation between the actual surface of the lens and the ideal surface it is designed to be, which can be a spherical, aspherical, diffractive, or flat surface. This error greatly affects the lens optical performance, as it causes aberrations, reducing the image or light quality obtained. Using the SPDT method with aluminum material for the SS, the author in [8] demonstrated that the FE of the sphere was reduced by half compared to previously used methods. The research results controlled by the STS (Slow Tool Servo) technique in SPDT [9] show that the form accuracy has reached the µm level.

There are many optimization algorithms such as the artificial bee colony (ABC) algorithm [10], ant colony optimization (ACO) algorithm [11], particle swarm optimization (PSO) algorithm [12]. PSO has advantages over other algorithms such as its simple structure and much easier implementation compared to other optimization algorithms. PSO parameters are usually

ISSN 2734-9381

https://doi.org/10.51316/jst.185.etsd.2025.35.4.6 Received: Feb 21, 2025; Revised: Mar 30, 2025 Accepted: Apr 2, 2025; Online: Sep 20, 2025. few and not too complex to adjust. PSO has the ability to find optimal solutions efficiently thanks to the cooperation between individuals in the search space. This algorithm typically converges quickly to the optimal solution vicinity. It can also be adjusted to enhance exploration capability (searching new areas) or exploitation (detailed search within an area) by tuning the parameters. This algorithm is used [13] to optimize energy consumption, and [14] to optimize the structural parameters of the Fiber Bragg Grating accelerometer.

This article focuses on constructing a regression equation for Al6061 sphere FE using response surface methodology (RSM) and the Box-Behnken (BB) model. PSO algorithm is used to optimize the FE and find the corresponding set of cutting parameter values. The paper structure is presented with the introduction section. Next, the model and research method are described in Section 2, in which the actual model along with the processing and measurement equipment system is considered together with a set of 15 experiments to collect the necessary information. Accordingly, some results were found and analyzed in detail in Section 3. Finally, the research results and their significance are summarized and presented in Section 4.

#### 2. Model and Research Method

#### 2.1. Research Model

The research was conducted on a super-precision lathe using diamond cutting tools to machine the Al6061 SS, employing the BB method and the PSO algorithm to achieve optimal FE based on optimizing the input technological parameters. The steps are described in the following steps:

## Step 1: Problem Identification

Input: Three factors technological parameters consisting: spindle speed n (rev/min) feed rate f (mm/min), and depth of cut ap ( $\mu$ m).

Process: Define the problem and establish the relationship between cutting parameters and FE.

Output: Build a regression model and find the cutting parameter set corresponding to the optimal FE value. From there, each parameters pair influence on the FE is also considered.

## Step 2: Experimental Model Construction

Input: Defined ranges (upper and lower limits) for technological parameters.

Process: Construct the coding table for the parameters and develop the experimental matrix using the BB method.

Output: Experimental design matrix for subsequent machining tests.

Step 3: Experimental Machining and Data Collection

Input: Experimental matrix from Step 2.

Process: Machine Al6061 spherical samples with 15 sets of cutting parameters on the SPDT machine. Measure the FE for each experiment.

Output: Dataset of FE values corresponding to each parameter set.

Step 4: Regression Model Development based on ANOVA

Input: Dataset obtained from Steps 2 and 3.

Process: Perform regression analysis and ANOVA to construct a mathematical model representing the relationship between cutting parameters and FE. Define the objective function.

Output: Regression model (objective function) describing FE.

Step 5: Optimization Using Particle Swarm Optimization

Input: the objective function from step 4, the limits of the parameters, and the algorithm parameters (MaxIt, npop, w, C1, C2).

Process: Initialize population; evaluate objective function for each individual; update velocity and position of individuals; identify the global best solution.

Output: Optimal cutting parameter set, corresponding minimum FE, and quantified influence of parameters on FE. The steps are described in Fig. 1.

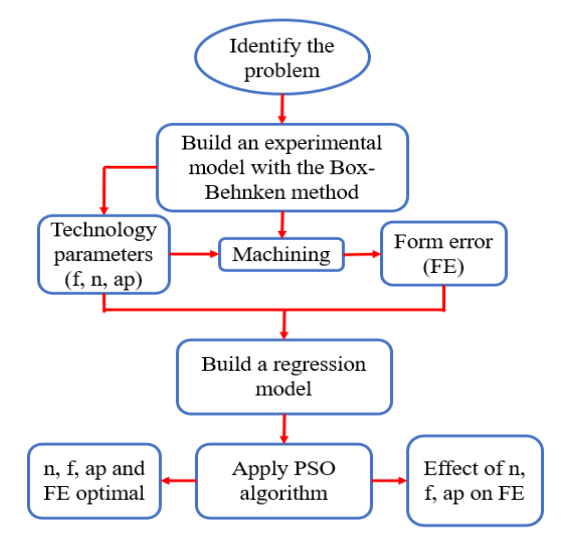


Fig. 1. Steps to implement the research content

## 2.2. Experiments and Measurements

The experiment was conducted on the ultra-precision lathe Nanoform®X. The FE was measured on the Form Talysurf® PGI Optics PRO profilometer (Fig. 2), which measures FE with high precision on the lens various surface types with a measurement range 20 mm and a resolution 0.2 nm. The experiment was conducted on an Al6061 billet (Fig. 3) with a diameter Ø30, a height is 20 mm, and a spherical radius is 19.5 mm, with the chemical composition shown in Table 1.

Table 1. Chemical composition of Al6061

Element	Mg	Si	Mn	Cu	Fe	Al	Other
wt.%	1.38	0.19	0.49	4.04	0.15	93.62	0.13

Table 2. Cutting tool specifications

Specifications	Cutting edge radius	Front angle	Cutting height	Rear angle	Included angle	Waviness
Dimensions	0.684 mm	-25°	7.475 mm	12°	60°	120°



Fig. 2. Form Talysurf measuring machine



Fig.4. Cutting tool

The cutting tool is the diamond turning tool NN60R0635mWGC-MS0454 (Fig. 4) with specifications shown in Tab. 2. The technology system (Fig. 5) includes a vacuum chuck, Al6061 workpiece, fixture, diamond turning tool, and mist cooling system.

The experiments are designed based on three input technological parameters suitable for the machine system and the tool's machining range. The chuck is adjusted so that the runout is less than 0.005  $\mu$ m for the most stable system.

## 2.3. Experimental Planning Model

The experiment was conducted based on the BB matrix, a type of experimental design in the field of RSM. This model was developed by George E. P. Box and Donald Behnken in 1960 [15], primarily used to construct a mathematical model describing the relationship between input factors (variables) and an output (response) to optimize the process. BB main characteristic is that it does not include points at the design space corners but focuses on the midpoints or the design space edges surfaces, helping to reduce the number of experiments compared to full factorial



Fig. 3. Spherical workpieces

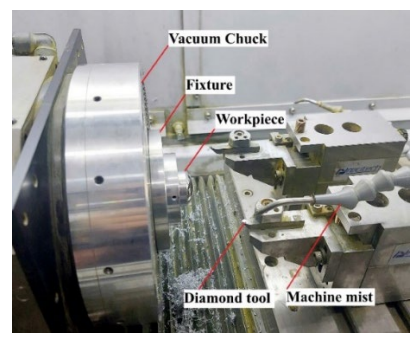


Fig. 5. Ultra-precision lathe system

designs (Fig. 6).

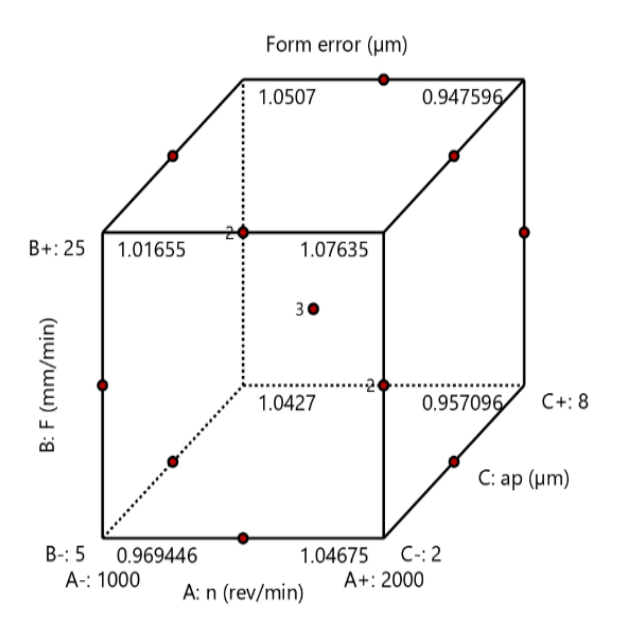


Fig. 6. The BB model experimental point distribution diagram

The equation has the form:

$$y = \beta_0 + \sum_{i=1}^k \beta_i x_i + \sum_{i=1}^k \beta_{ii} x_i^2 + \sum_{i < j} \beta_{ij} x_i x_j$$
 (1)

where y is the response,  $x_i$  is the independent variables,  $\beta$  is the regression coefficients.

Since BB saves time and resources compared to other designs, especially when variables number is large, and due to not using experiments at the vertex points, BB reduces variables risk exceeding experimental limits. This model is ideal when the relationship between

input and output factors is nonlinear, and BB allows for the estimation of quadratic and interaction coefficients with accuracy equivalent to or better than CCD, while requiring fewer runs. Therefore, the BB model is used to find the optimal value for the FE. The cutting parameters are divided into 3 levels with the coding levels shown in Table 3.

Through the machining and measurement process, the deformation error results corresponding to each set of input technological parameters are obtained. The BB model experimental matrix corresponding to the three parameters n (rev/min), f (mm/min), ap ( $\mu$ m) and the corresponding results are presented in Table 4.

Table 3. Values the experimental variables coding levels

Cll	Danamatana	TT:4	Levels		
Symbol	Parameters	Unit -	1 (-1)	2 (0)	3 (1)
$x_1$	Spindle speed (n)	rev/min	1000	1500	2000
$x_2$	Feed rate (f)	mm/min	5	15	25
<i>x</i> <sub>3</sub>	Depth of cut (ap)	μm	2	5	8

Table 4. Experiment matrix and experimental results

I	Encryption value	Result	
n (rev/min)	f (mm/min)	ap (µm)	FE (μm)
-1	-1	0	1.0011
1	-1	0	1.003
-1	1	0	1.0388
1	1	0	1.0232
-1	0	-1	1.0156
1	0	-1	1.0781
-1	0	1	1.0743
1	0	1	0.9739
0	-1	-1	0.9592
0	1	-1	1.0025
0	-1	1	0.9611
0	1	1	0.9502
0	0	0	1.0087
0	0	0	1.0087
0	0	0	0.9743
	n (rev/min)  -1  1  -1  1  -1  1  -1  1  0  0  0  0  0  0	-1 -1 1 -1 -1 1 -1 1 -1 0 -1 0 -1 0 -1 0	$n$ (rev/min) $f$ (mm/min) $ap$ ( $\mu$ m)           -1         -1         0           1         -1         0           -1         1         0           -1         0         -1           1         0         -1           -1         0         1           1         0         1           0         -1         -1           0         1         -1           0         1         1           0         1         1           0         0         0           0         0         0           0         0         0

## 2.4. PSO Swarm Algorithm

PSO is an optimization method based on evolutionary algorithms, proposed by Eberhart and Kennedy in 1995 [16]. PSO is inspired by the behavior of bird flocks and fish schools when they forage or move together. This is a global optimization algorithm, widely used in artificial intelligence field and computer science to solve non-linear and non-smooth optimization problems. PSO simulates the behavior of a individuals group in the search space to find the optimal solution. Each individual represents a potential solution and has key attributes including: position, velocity, personal best position history, and swarm best position history. The steps to implement the PSO algorithm are as follows:

Step 1: Start (initialize the algorithm)

#### Step 2: Initialize the population

Build the population size I (number of individuals), algorithm iterations maximum number (T), search space dimensions' number.

## Step 3: Calculate the objective function

For each individual, calculate the objective function value at the current position.

Step 4: Create a search loop

## Step 5: Update velocity and position

In each iteration, the individual updates its velocity based on the trajectory towards the best position it has ever achieved and the trajectory towards the best position the entire swarm has ever achieved. Each individual velocity is updated based on its own best position (pBest) and the swarm best position (gBest). The formula for the individual velocity i at iteration t+1 is:

$$v_{i}(t+1) = \omega v_{i}(t) + c_{1} x_{1} \cdot (pBest_{i} - x_{i}(t)) + c_{2} x_{2} \cdot (gBest - x_{i}(t))$$
(2)

where  $v_i(t)$  is velocity of individual i at time t;  $\omega$  is inertia weight, usually ranging from 0.4 to 0.9, helps control the previous velocity influence;  $c_1$  is cognitive coefficient, adjusting the personal best position influence level pBest;  $c_2$  is social coefficient, adjusting the best position influence level in the herd gBest;  $r_1$ ,  $r_2$  are random numbers in the range [0,1] which help create randomness in the velocity update process; pBest is the best personal position of individual i up to the present time; gBest is the best position in the herd among all individuals;  $x_i(t)$  is current position of individual i at time t.

The position of each individual is updated by adding its new velocity to the current position:

$$x_i(t+1) = x_i(t) + v_i(t+1)$$
 (3)

where:

 $x_i(t)$ : current position of individual i at time t

 $v_i(t+1)$ : speed of individual i after the update at time t+1

Step 6: Update pBest và gBest best value

Compare the current position objective function value with pBest. If better, update pBest to the current position. Compare the pBest to update, if any pBest is better than gBest, then update gBest.

Step 7: Check stop conditions

Step 8: Stop searching and output the results

The PSO algorithm will stop when the final result is achieved (maximum number of iterations).

The algorithm diagram is described in Fig. 7.

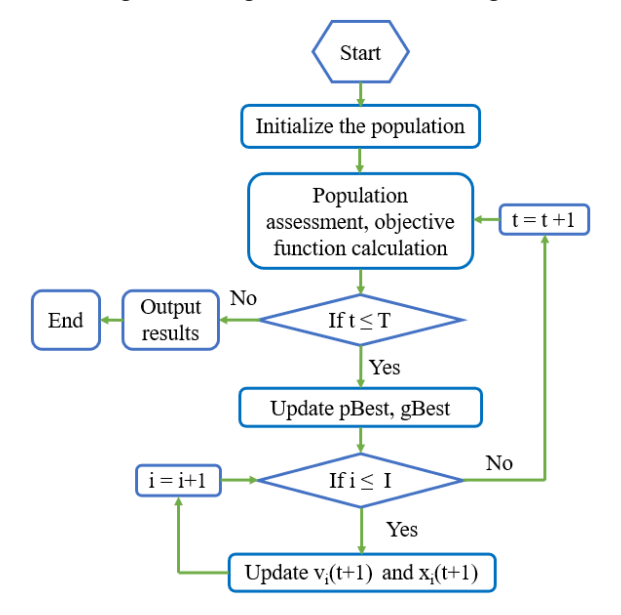


Fig. 7. PSO algorithm diagram

## 3. Results and Discussion

## 3.1. ANOVA Analysis and Regression Model

Using the specialized software Design Expert to construct the regression equation and observe the model's fit analysis results with the experiment,  $R^2 = 0.9428$  (R-Squared) close to 1 indicates high reliability, proving that the experimental results are close to the model's predicted values. Adeq Precision equal 10.3, which is greater than 4, indicates that the model has reliable predictive capability.

Table 5 describes the ANOVA analysis results and the regression equation coefficients. The *F*-value column indicates the regression model fit goodness, showing the differences in variance among mean values groups. A high *F*-value indicates that the model has a

better ability to explain the variation in the data compared to a model without any influencing factors. If the *F*-value is large and the *P*-value is less than 0.05, the model is considered significant. With an *F*-value of 9.16 and the model being statistically significant with high reliability (*p*-value equal 0.0126 is less than 0.05), this proves that the model is fully compatible with the experiment. The FE column shows the regression equation coefficients. Corresponding to the significant

values in the *P*-value column are the coefficients that have a large influence on the form accuracy, the remaining values have little or no influence on the form accuracy. The FE regression equation is obtained as follows:

$$FE = 0,9972 - 0,0139x_3 - 0,0407x_1x_3 + 0,0414x_1^2 - 0,0221x_2^2 (\mu m)$$
 (4)

Table 5. ANOVA analysis results and the regression coefficients

Source	Sum of Squares	df	Mean Square	<i>F</i> -value	P-value	Significance	Form error =
Model	0.0184	9	0.0020	9.16	0.0126	Significant	+0.9972
A-n	0.0003	1	0.0003	1.49	0.2769	Not Significant	-0.0065 × A
B-F	0.0007	1	0.0007	3.16	0.1356	Not Significant	+0.0094×B
C-ap	0.0015	1	0.0015	6.89	0.0469	Significant	-0.0139×C
AB	0.0001	1	0.0001	0.3424	0.5839	Not Significant	-0.0044× AB
AC	0.0066	1	0.0066	29.67	0.0028	Significant	-0.0407×AC
ВС	0.0004	1	0.0004	1.71	0.2480	Not Significant	-0.0098×BC
A2	0.0063	1	0.0063	28.26	0.0032	Significant	$+0.0414 \times A2$
B2	0.0018	1	0.0018	8.05	0.0364	Significant	$-0.0221 \times B2$
C2	0.0000	1	0.0000	0.1617	0.7042	Not Significant	-0.0031×C2
Residual	0.0011	5	0.0002				
Lack of Fit	0.0003	3	0.0001	0.2782	0.8402	Not Significant	
Pure Error	0.0008	2	0.0004				
Cor Total	0.0196	14					

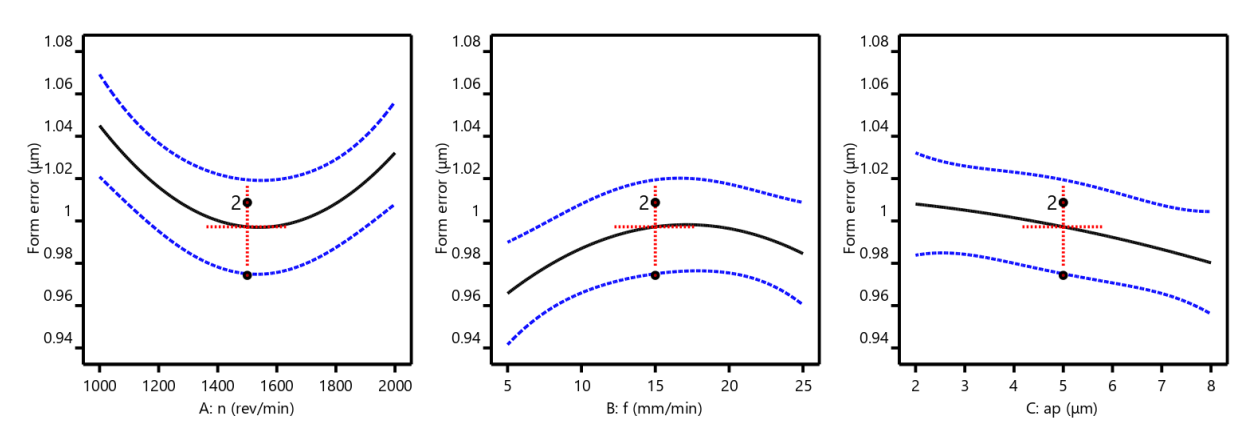


Fig. 8. Technological parameters' influence on FE

## 3.2. Results of Establishing the Prediction Model and Optimal Value

The objective function is a mathematical equation that represents the relationship between technological parameters and FE, finding the optimal technological parameters for optimal FE. The regression equation (2) has been constructed from the BB model.

The technological limits are  $-1 \le x_1, x_2, x_3 \le 1$  corresponding to  $1000 \le n \le 2000$  (rev/min),  $5 \le f \le 25$  (mm/min),  $2 \le ap \le 8$  ( $\mu$ m). The PSO main parameters establish in MATLAB software are shown in Table 6.

The FE optimal result is described in Fig. 9. The optimal FE value achieved is 0.95  $\mu$ m with the encoded technological parameter set as  $x_1$  equal 0.4915,  $x_2$  equal -1,  $x_3$  equal 1 corresponding to the input parameters

n equal 1746 (rev/min), f equal 5 (mm/min), ap equal 8 ( $\mu$ m).

Table 6. PSO algorithm parameters

No	Parameters	Symbol	Value
1	Search iterations number	MaxIt	100
2	Swarm population size	npop	100
3	Inertia coefficient	W	1
4	Individual acceleration coefficient	C1	2
5	Population acceleration coefficient	C2	2

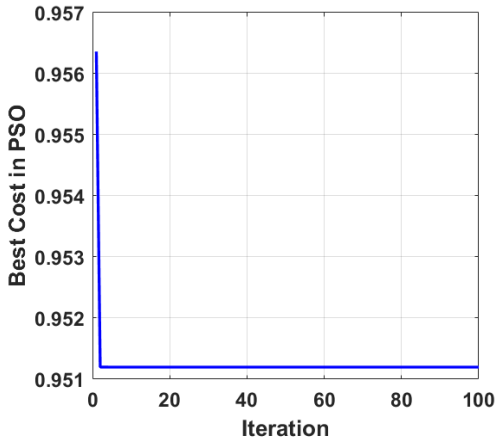


Fig. 9. The optimal FE value

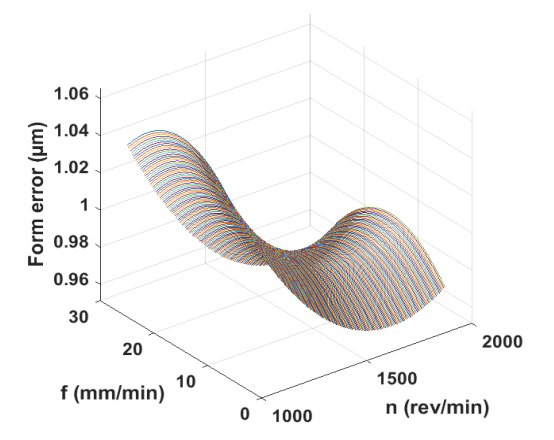


Fig. 10. The influence of n and f

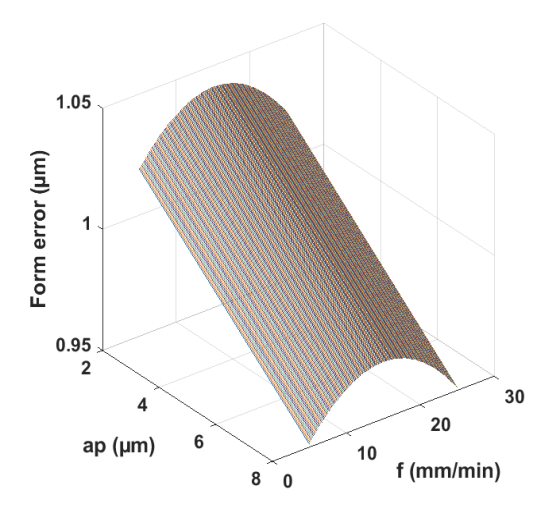


Fig. 11. The influence of ap and f

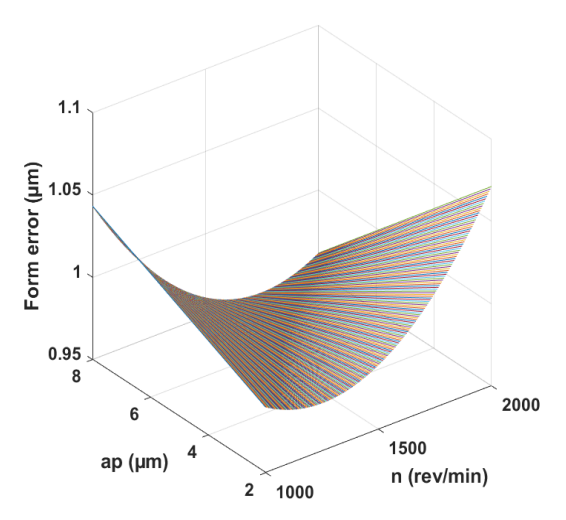


Fig. 12. The influence of *ap* and *n* 

Machining Al6061 under varying input parameters produces different FE. Fig. 10, Fig. 11, and Fig. 12 show how the three parameters influence FE. The cutting speed at f equal to 15 mm/min (Fig. 10, Fig. 11) has the largest FE, the FE decreases as the cutting speed becomes smaller or larger (parabola). When using UPT on the lens surface, low feed speed should be selected to reduce vibration, increase accuracy, improve surface quality while the FE still reaches a small value. The depth of cut increases, the FE decreases (Fig. 11) because a low depth of cut (the micrometer range) results in low cutting forces, causing sliding on the surface without actual cutting, leading to wear and deformation. Low cutting force may not exceed the elastic limit of the workpiece, causing it to bounce during cutting and resulting in FE. However, with a small depth of cut and low spindle speed, the tool interacts with the workpiece for a longer time, allowing the cutting force to be more effective in material removal rather than causing sliding (Fig. 12). The spindle speed depends on the depth of cut and the feed rate, for each pair of feed rates and depth of cut, there will be different optimal spindle speeds due to UPT with very small cutting parameters f and ap.

It can be seen that in UPT, it is necessary to consider many factors such as the workpiece material to choose an appropriate depth of cut to avoid tool slipping, along with the spindle speed and feed rate to achieve the best form accuracy. In cases where it is necessary to choose a depth of cut that is too small, which may cause slipping, the spindle speed should be reduced appropriately to achieve the best form accuracy. However, the spindle speed should not be reduced too much, as it may not generate enough kinetic energy to overcome the initial cutting resistance of the workpiece, still resulting in significant FE.

#### 4. Conclusion

The research applied the BB method to construct the experimental model, while also using the PSO algorithm to optimize the input technological parameters for the UPT Al6061 SS. Through analysis and optimization, the parameters including spindle speed, feed rate, and depth of cut have been determined with optimal values, helping to minimize FE. The results show the following:

- 1. The actual model established using the BB method has high accuracy, showing that the predicted and actual results are not significantly different, demonstrating the reliability of the model.
- 2. The PSO algorithm has optimized the input parameters effectively, a quick convergence time and the ability to achieve global optimal results. The FE reached an optimal value 0.95 (µm) corresponding to the technological parameters n equal 1746 (rev/min), f equal 5 (mm/min), ap equal 8 (μm), indicating the method great potential in improving the quality of SS UPM.

3. The influence of technological parameters is analyzed in detail, attention to the workpiece material to select an appropriate depth of cut to avoid slipping that causes significant FE. A low feed rate selection should be prioritized, which in turn determines the spindle speed to match the depth of cut and feed rate.

## Acknowledgments

This research is funded by Vietnam National Foundation Science and Technology Development (NAFOSTED) under grant number 107.01-2020.15.

#### References

- Y. Cai, Y. Yang, Y. Wang, R. Wang, X. Zhu, R. Kang, Model for surface topography prediction in the ultraprecision grinding of silicon wafers considering volumetric errors, Measurement, vol. 234, pp. 114825,
  - https://doi.org/10.1016/j.measurement.2024.114825
- Z. Xu, L.W.S. Yip, S. To, Condition monitoring of threeaxis ultra-precision milling machine tool for anomaly detection, Procedia CIRP, vol. 119, pp.1210-1215, 2023 https://doi.org/10.1016/j.ijmachtools.2024.104219
- C. Liu, J. Ke, T. Yin, W.S. Yip, J. Zhang, S. To, J. Xu, Cutting mechanism of reaction-bonded silicon carbide in laser-assisted ultra-precision machining, International Journal of Machine Tools and Manufacture, vol. 203, pp. 104219, Dec. 2024. https://doi.org/10.1016/j.ijmachtools.2024.104219
- H. Gong, S. Ao, K. Huang, Y. Wang, and C. Yan, Tool path generation of ultra-precison diamond turning: a state-of-the-art review, Nanotechnology and Precision Engineering, vol. 2, iss. 3, pp. 118-124, Sep. 2019 https://doi.org/10.1016/j.npe.2019.10.003
- Z. Zheng, Design of off-axis reflective projection lens using spherical Fresnel surface, Optik, vol. 122, iss. 2, pp. 145-149, Jan. 2011. https://doi.org/10.1016/j.ijleo.2010.02.011
- P. Gu, J. Chen, W. Huang, Z. Shi, X. Zhang, L. Zhu, Evaluation of surface quality and error compensation for optical aspherical surface grinding, Journal of Materials Processing Technology, vol. 327, pp. 118363, Jun. 2024. https://doi.org/10.1016/j.jmatprotec.2024.118363
- A.S. Garcia, L.M. Sanchez-Brea, J.d. Hoyo, F.J. Torcal-Milla, J.A. Gomez-Pedrero, Fourier series diffractive lens with extended depth of focus, Optics & Laser Technology, vol. 164, pp. 109491, Sep. 2023. https://doi.org/10.1016/j.optlastec.2023.109491
- Y. Huang, B. Fan, Y. Wan, S. Li, Improving the performance of single point diamond turning surface with ion beam figuring, Optik - International Journal for Light and Electron Optics, vol. 172, pp. 540-544, Nov. 2018. https://doi.org/10.1016/j.ijleo.2018.07.039
- V. Mishra, N. Kumar, R. Sharma, H. Garg, V. Karara, Development of aspheric lenslet array by slow tool servo machining, Materials Today: Proceedings, vol. 24, part 2, pp. 1602-1607, 2020. https://doi.org/10.1016/j.matpr.2020.04.481

## JST: Engineering and Technology for Sustainable Development

Volume 35, Issue 4, October 2025, 043-051

- [10] S.F. Hussain, A. Pervez, M. Hussainb, Co-clustering optimization using artificial bee colony (ABC) algorithm, Applied Soft Computing Journal, vol. 97, part B, pp. 106725, Dec. 2020. https://doi.org/10.1016/j.asoc.2020.106725
- [11] F. Huo, S. Zhu, H. Dong, W. Ren, A new approach to smooth path planning of Ackerman mobile robot based on improved ACO algorithm and B-spline curve, Robotics and Autonomous Systems, vol. 175, pp. 104655, May. 2024. https://doi.org/10.1016/j.robot.2024.104655
- [12] J. Wang, Z. Li, C. Pan, Energy-efficient trajectory planning with curve splicing based on PSO-LSTM prediction, Control Engineering Practice, vol. 150, pp. 106009, Sep. 2024. https://doi.org/10.1016/j.conengprac.2024.106009
- [13] G.V. Priya, S. Ganguly, Multi-swarm surrogate model assisted PSO algorithm to minimize distribution network energy losses, Applied Soft Computing, vol. 159, pp. 111616, Jul. 2024. https://doi.org/10.1016/j.asoc.2024.111616
- [14] W. Mo, Z. He, C. Xing, Z. Yu, A flexible hinge FBG accelerometer based on PSO algorithm, Optical Fiber Technology, vol. 87, pp. 103905, Oct. 2024. https://doi.org/10.1016/j.yofte.2024.103905
- [15] Montgomery D.C., Design and Analysis of Experiments, Technometrics, pp. 158, Jan. 2012. https://doi.org/10.1198/tech.2006.s372
- [16] J. Kennedy and R. Eberhart, Particle swarm optimization in Proceedings of ICNN'95 – International Conference on Neural Networks, Perth, WA, Australia, pp. 1942–1948, 27 Nov. 1995 - Dec. 1995. https://doi.org/10.1109/ICNN.1995.488968